

ENHANCED GLUTAMATERGIC PHENOTYPE OF MESENCEPHALIC DOPAMINE NEURONS AFTER NEONATAL 6-HYDROXYDOPAMINE LESION

G. DAL BO,^a N. BÉRUBÉ-CARRIÈRE,^b J. A. MENDEZ,^a D. LEO,^a M. RIAD,^b L. DESCARRIES,^{b,c,d} D. LÉVESQUE^e AND L.-E. TRUDEAU^{a,d*}

^aDepartment of Pharmacology, Faculty of Medicine, Université de Montréal, C.P. 6128, Succursale Centre-Ville, Montréal, QC, Canada H3C 3J7

^bDepartment of Pathology and Cell Biology, Université de Montréal, C.P. 6128, Succursale Centre-Ville, Montréal, QC, Canada H3C 3J7

^cDepartment of Physiology, Faculty of Medicine, Université de Montréal, C.P. 6128, Succursale Centre-Ville, Montréal, QC, Canada H3C 3J7

^dGroupe de Recherche sur le Système Nerveux Central, Université de Montréal, C.P. 6128, Succursale Centre-Ville, Montréal, QC, Canada H3C 3J7

^eFaculty of Pharmacy, Université de Montréal, C.P. 6128, Succursale Centre-Ville, Montréal, QC, Canada H3C 3J7

Abstract—There is increasing evidence that a subset of mid-brain dopamine (DA) neurons uses glutamate as a co-transmitter and expresses vesicular glutamate transporter (VGLUT) 2, one of the three vesicular glutamate transporters. In the present study, double *in situ* hybridization was used to examine tyrosine hydroxylase (TH) and VGLUT2 mRNA expression during the embryonic development of these neurons, and postnatally, in normal rats and rats injected with 6-hydroxydopamine (6-OHDA) at P4 to destroy partially DA neurons. At embryonic days 15 and 16, there was a regional overlap in the labeling of TH and VGLUT2 mRNA in the ventral mesencephalon, which was no longer found at late embryonic stages (E18–E21) and postnatally. In normal pups from P5 to P15, only 1–2% of neurons containing TH mRNA in the ventral tegmental area (VTA) and substantia nigra, pars compacta, also displayed VGLUT2 mRNA. In contrast, after the cerebroventricular administration of 6-OHDA at P4, 26% of surviving DA neurons in the VTA of P15 rats expressed VGLUT2. To search for a colocalization of TH and VGLUT2 protein in axon terminals of these neurons, the nucleus accumbens of normal and 6-OHDA-lesioned P15 rats was examined by electron microscopy after dual immunocytochemical labeling. In normal rats, VGLUT2 protein was found in 28% of TH positive axon terminals in the core of nucleus accumbens. In 6-OHDA-lesioned rats, the total number of TH positive terminals was considerably reduced, and yet the

proportion also displaying VGLUT2 immunoreactivity was modestly but significantly increased (37%). These results lead to the suggestion that the glutamatergic phenotype of a VTA DA neurons is highly plastic, repressed toward the end of normal embryonic development, and derepressed postnatally following injury. They also support the hypothesis of co-release of glutamate and DA by mesencephalic neurons *in vivo*, at least in the developing brain. © 2008 IBRO. Published by Elsevier Ltd. All rights reserved.

Key words: dopamine, glutamate, VGLUT2, 6-OHDA, mesencephalon, nucleus accumbens.

The dopamine (DA) system is known to be critical for motor control and many aspects of cognition. It is implicated in Parkinson's disease and neuropsychiatric disorders, including schizophrenia and addiction. In the last 10 years, considerable evidence has accrued for glutamate co-transmission by central DA neurons. For example, release of glutamate was demonstrated to occur at autapses established by isolated DA neurons in culture (Sulzer et al., 1998; Bourque and Trudeau, 2000; Joyce and Rayport, 2000) and stimulation of presumed DA neurons in the ventral tegmental area (VTA) was shown to evoke glutamatergic synaptic responses in neurons of the nucleus accumbens (nAcb) and prefrontal cortex (Chuhma et al., 2004; Lavin et al., 2005). In addition, mesencephalic DA neurons in culture were shown to express vesicular glutamate transporter (VGLUT) 2 (Dal Bo et al., 2004), one of the three VGLUTs (Ni et al., 1995; Bellocchio et al., 1998; Hisano et al., 2000; Aihara et al., 2000; Herzog et al., 2001; Freneau et al., 2001; Varoqui et al., 2002; Gras et al., 2002).

In two recent *in situ* hybridization studies, expression of VGLUT2 mRNA by mesencephalic DA neurons has been demonstrated in intact tissue (Kawano et al., 2006; Yamaguchi et al., 2007). In the first study, the authors reported that as much as 19% of tyrosine hydroxylase (TH) immunopositive neurons of the VTA (A10 cell group) also expressed VGLUT2 mRNA (Kawano et al., 2006). In the second study, the authors found that only 0.1% of neurons expressing TH mRNA in this region also contained VGLUT2 mRNA (Yamaguchi et al., 2007). This large difference in proportion remains to be explained, but could reflect technical differences in experimental approach. In any case, both studies indicated a striking difference between *in vivo* and *in vitro* data, since a majority (80%) of isolated mesencephalic DA neurons in culture have been shown to express VGLUT2 (Dal Bo et al., 2004). In line with previous results demonstrating plasticity of the transmitter phenotype of neurons during development and in response to changes in neuronal activity (Furshpan

*Correspondence to: L.-E. Trudeau, Department of Pharmacology, Faculty of Medicine, Université de Montréal, C.P. 6128, Succursale Centre-Ville, Montréal, QC, Canada H3C 3J7. Tel: +1-514-343-5692; fax: +1-514-343-2291.

E-mail address: louis-eric.trudeau@umontreal.ca (L.-E. Trudeau).
Abbreviations: ANOVA, analysis of variance; DA, dopamine; DAB, 3,3'-diaminobenzidine tetrahydrochloride; Dig, digoxigenin; nAcb, nucleus accumbens; PBS, phosphate-buffered saline; PFA, paraformaldehyde; RH, random hexamer; RLi, rostral linear nucleus; SN, substantia nigra; SNC, substantia nigra pars compacta; TBS, Tris-saline buffer; TH, tyrosine hydroxylase; VGLUT, vesicular glutamate transporter; VTA, ventral tegmental area; 6-OHDA, 6-hydroxydopamine.

et al., 1976; Borodinsky and Spitzer, 2007; Borodinsky et al., 2004; Yang et al., 2002; Gillespie et al., 2005; Trevino and Gutierrez, 2005; Gutierrez and Heinemann, 2006; Gomez-Lira et al., 2005), this discrepancy between the *in vivo* and *in vitro* data is best resolved by hypothesizing that VGLUT2 expression in DA neurons is regulated during development, and may be up-regulated in response to trauma, such as tissue dissociation and culture or a partial lesion *in vivo*.

To investigate the glutamatergic phenotype of developing mesencephalic DA neurons *in vivo*, we used double *in situ* hybridization for TH mRNA and each subtype of VGLUT transcripts in pre- and postnatal rats, as well as double labeling immuno-electron microscopy with specific antibodies against TH and VGLUT2 in 15 day-old pups. Intact rats as well as rats subjected to neonatal i.c.v. administration of the neurotoxin 6-hydroxydopamine (6-OHDA) were examined in order to evaluate the effects of an early injury on the transmitter phenotype of surviving DA neurons.

We confirm that a small subset of mesencephalic DA neurons selectively expresses VGLUT2 mRNA, but not VGLUT1 or VGLUT3, and suggest that the glutamatergic phenotype of these neurons is repressed during late embryonic development and may be up-regulated in response to early postnatal injury. By visualizing both TH and VGLUT2 proteins in the same axon terminals of the nAcb, we also provide strong evidence for the capacity of mesencephalic DA neurons to release both DA and glutamate *in vivo*, at least in developing brain.

EXPERIMENTAL PROCEDURES

Animals

All procedures involving animals and their care were conducted in strict accordance with the Guide to the Care and Use of Experimental Animals (Ed2) of the Canadian Council on Animal Care. The experimental protocols were approved by the animal ethics committee (CDEA) of the Université de Montréal and conformed to international guidelines on the ethical use of animals, such as those of the Canadian Council on Animal Care. Care was also taken to minimize the number of animals used and their suffering. Sprague–Dawley male rats and pregnant dams were purchased from Charles River (Montreal, QC, Canada) and housed at a constant temperature (21 °C) and humidity (60%), under a fixed 12-h light/dark cycle, with free access to food and water.

Neonatal 6-OHDA lesions

Neonatal 6-OHDA lesions were produced as previously described (Stachowiak et al., 1984; Jackson et al., 1988; Fernandes Xavier et al., 1994). Four day-old pups received an s.c. injection of desipramine (50 μ l, 5.6 mg/ml in aCSF) (Sigma Chemical, St. Louis, MO, USA) 45 min before toxin injection, to protect noradrenergic neurons. The toxin (6-OHDA hydrochloride, Sigma), was dissolved (10 mg/ml) in aCSF containing 0.2% ascorbic acid to prevent oxidation. Pups were anesthetized on ice, placed on a cold body mold, and administered 5 μ l of 6-OHDA solution in each lateral brain ventricle (stereotaxic coordinates: L \pm 1.5 mm, AP 0 mm to Bregma, and V 3.3 mm below the dura), at a rate of approximately 1.5 μ l/min. The intraventricular injections were made with a 30-gauge needle attached to a 10 μ l Hamilton syringe. The syringe was left in place for 3 min after each injection. Sham controls were injected with vehicle under the same conditions. The pups were then warmed in a humidified box and re-

turned to their mother 2 h later. They were maintained with their mother until sacrifice, 11 days post-surgery (at P15).

Double *in situ* hybridization

The double *in situ* hybridization technique (Beaudry et al., 2000) was used in rat embryos as well as in normal P5, P10 and P15 rat pups, and in 6-OHDA-lesioned P15 rats and their sham controls (Cossette et al., 2004; St-Hilaire et al., 2005). The embryos were removed from gestating dams under isoflurane anesthesia (isoflurane 2%, O₂ 1.8 l/min), on days 14, 15, 18 and 21 of gestation. They were immersed in frozen isopentane, and stored at –80 °C until used. The postnatal rats were anesthetized with halothane and their brain was quickly dissected out, immersed in cold phosphate-buffered saline (PBS, 50 mM, pH 7.4), and cut in two parts at the level of the median eminence. The rostral part containing the striatum was fixed by immersion in 4% paraformaldehyde (PFA) solution for 48 h and processed for TH immunohistochemistry as described below. The caudal part containing the mesencephalon was immersed in frozen isopentane and stored at –80 °C until used.

[³⁵S]UTP-labeled VGLUT1, 2 or 3 probes, and a nonradioactive digoxigenin (Dig)-labeled TH probe were prepared as follows. Complementary RNA (cRNA) probes for each VGLUT subtype were synthesized from pCRII-Topo plasmids containing a fragment of each VGLUT cDNA. cDNA fragment sizes were 519, 539 and 415 base pairs for VGLUT1, 2 and 3, respectively (Herzog et al., 2001; Gras et al., 2002). Antisense probes were produced by linearization of the plasmid using the *NotI* restriction enzyme and SP₆ polymerase, and synthesized with the Promega riboprobe kit (Promega, Madison, WI, USA) and [³⁵S]UTP (Perkin-Elmer, Mississauga, ON, Canada). For sense probes, the *HindIII* restriction enzyme was used to linearize the plasmid, and probes were synthesized with T₃ polymerase. Labeled probes were purified with mini QuickSpin RNA columns (Roche Diagnostics, Laval, QC, Canada). The Dig-labeled TH probe was generated as previously described (Cossette et al., 2004). Both Dig-labeled TH (20 ng/ μ l) and specific radioactive-labeled VGLUT probes (2 \times 10⁶ CPM) were included simultaneously in the hybridization solution.

Transverse sections of the mesencephalon (12 μ m-thick) were cut with a cryostat, mounted on Superfrost Plus slides (Fisher Scientific, Toronto, ON, Canada), and stored at –80 °C until used. Before hybridization, slides were fixed in 4% PFA for 20 min and rinsed three times in PBS. *In situ* hybridization was performed overnight at 58 °C. To reduce non specific Dig labeling, an additional step was added to standard post-hybridization treatments: immersion in a 50% formamide solution in 2 \times saline–sodium citrate buffer (SSC, 300 mM NaCl, 30 mM sodium citrate, pH 7 in DEPC water) for 30 min at 60 °C. The slides were then immersed for 30 min in blocking solution containing 2% BSA and 0.3% Triton X-100 in buffer A solution (100 mM Tris–HCl, pH 7.5 and 150 mM NaCl), covered with 100 μ l of an anti-Dig antibody conjugated to alkaline phosphatase (Roche Diagnostics) diluted 1/200 in buffer A, and placed at 4 °C overnight. After three rinses (10 min) in buffer A, the Dig was revealed in buffer B (100 mM Tris–HCl, pH 9.5, 100 mM NaCl and 50 mM MgCl₂) containing 0.4 mM nitroblue tetrazolium chloride, 0.45 mM 5-bromo-4-chloro-3-indolyl phosphate (Dig detection kit, Roche Diagnostic) and 1 mM levamisole, for 30 min at room temperature, in the dark. The Dig reaction was stopped by immersion in buffer C (100 mM Tris–HCl, pH 8 and 1 mM EDTA). After three additional washes with distilled water, slides were air-dried, and apposed against BiomaxMR radioactive-sensitive film (Kodak, New Haven, CT, USA) for 3 days. Following film exposition, the slides were coated by dipping with LM-1 photographic emulsion (Amersham, ON, Canada), stored in the dark for 21 days at 4 °C, developed in D-19 (Kodak) and coverslipped with a water-soluble mounting medium (Permafluor; Lipshaw Immunon, Pittsburgh, PA, USA). Slides used to compare the dual labeling at different ages and/or be-

between experimental conditions were systematically processed together. All these sections were examined under bright-field illumination with an Olympus IX-50 microscope (Carsen Group, Markham, ON, Canada), at 400× magnification.

In sections from embryos, the contour of individual neurons could not be distinguished after the above processing for dual *in situ* hybridization. To quantify *in situ* hybridization signals, counts of silver grains (VGLUT2 mRNA) were therefore obtained from tissue areas also displaying Dig positivity (TH mRNA). This was done with the aid of the public domain Image J software (NIH) in images captured with an ORCA-II cooled digital camera (Hamamatsu, Bridgewater, NJ, USA). In each section, silver grain counts were obtained from three square areas ($\pm 6000 \mu\text{m}^2$ each) of the ventral mesencephalon displaying Dig positivity, and three areas of the same sections ($\pm 5600 \mu\text{m}^2$ each) showing only weak, silver grain labeling (background). The counts from TH-Dig positive areas were then averaged at each embryonic age, and expressed in number of grains per $500 \mu\text{m}^2$ (an area corresponding to a cluster of DA neurons cell bodies), after subtracting the background (0.9–1.9 silver grains per $500 \mu\text{m}^2$ of section). This analysis was performed in three or four sections per embryo, and three embryos each at E15 and E18, and five embryos each at E16 and E21.

In sections from postnatal rats, background labeling was similarly measured and found at 0.37–0.53 silver grains per $500 \mu\text{m}^2$ of section. As in previous studies (Kawano et al., 2006), TH-Dig positive cells (DA neurons) were considered to be labeled for VGLUT2 mRNA if displaying three times the background level, i.e. at least six silver grains per cell body (Gratto and Verge, 2003). In four rats of each experimental condition tested and three or four sections per rat, located between stereotaxic planes -5.28 mm and -6.24 mm from Bregma in adult rats (Paxinos and Watson, 2005), singly and doubly labeled cells were then counted visually.

TH immunohistochemistry

TH immunohistochemistry was used to verify the extent of 6-OHDA lesions. After 48 h of fixation in PFA, $24 \mu\text{m}$ -thick transverse sections of the forebrain were cut with a VT1000s vibratome (Leica Microsystems, Nussloch, Germany), rinsed in PBS ($3 \times 10 \text{ min}$) and then incubated in 5% goat serum solution containing 10% BSA and 0.1% Triton X-100 for 1 h, in order to block non-specific labeling. Sections across the striatum were incubated overnight in mouse monoclonal TH antibody (Clone TH-2, Sigma) diluted 1/1000 in PBS. The signal was detected with biotinylated anti-mouse antibodies (Jackson ImmunoResearch, West Grove, PA, USA) diluted 1/1000, followed by 1/1000 streptavidin–HRP (Jackson). After $3 \times 10 \text{ min}$ washes in PBS, followed by $2 \times 10 \text{ min}$ washes in Tris–HCl (50 mM, pH 7.4), the peroxidase reaction was revealed with 0.05% 3,3'-diaminobenzidine tetrahydrochloride (DAB; Sigma) and hydrogen peroxide (0.01%) in Tris–HCl. The DAB reaction was stopped by immersion in Tris–HCl.

RT-mPCR

Transverse slices ($\sim 1 \text{ mm}$ thickness) of the mesencephalon, cut by hand at the level of the VTA and substantia nigra (SN), were isolated from the frozen brain of normal, sham-injected and 6-OHDA-lesioned, 15 day-old rats ($n=3$ in each group). The slices were trimmed under the microscope to keep only the VTA and SN pars compacta (SNc). Total RNA was extracted from each individual sample using TRIzol[®] Reagent (Invitrogen, Burlington, ON, Canada), according to the manufacturer's instructions. All samples were stored at $-80 \text{ }^\circ\text{C}$ until used. Reverse transcription was performed on $2.5 \mu\text{g}$ of total RNA for 1 h at $37 \text{ }^\circ\text{C}$ with 0.5 mM dNTPs mix (Qiagen), $2.5 \mu\text{M}$ random hexamers (RH) (Applied Biosystems, CA, USA) and 100 U M-MLV reverse transcriptase (Invitrogen). Reaction was stopped by heating at $70 \text{ }^\circ\text{C}$ for 15 min, then multiplex-semiquantitative PCR amplification was performed

using 10% of the RT reaction, $2.5 \mu\text{l}$ $10 \times$ PCR buffer, $0.5 \mu\text{l}$ of 100 mM dNTPs, 2.5 U of *Taq* polymerase (all from Quiagen, ON, Canada), 1.5 mM MgCl_2 , and 10 pmol of each primer. Twenty-seven cycles were carried out as follows: denaturation at $94 \text{ }^\circ\text{C}$ for 60 s, annealing at $55 \text{ }^\circ\text{C}$ for 30 s and extension at $72 \text{ }^\circ\text{C}$ for 30 s. Amplification products were analyzed by 1.6% agarose gel electrophoresis. Band intensities were evaluated with Kodak ID v3.6.0 software.

Multiplex single-cell RT-PCR

Cells dissociation was performed following a protocol modified from Puma et al., (2001). Briefly, the ventral mesencephalon was dissected from E15 embryos and collected in ice-cold PBS supplemented with 6 mg/ml glucose. The tissue was treated with papain (Worthington Biochemical Corporation, Lakewood, NJ, USA) for 20 min at $37 \text{ }^\circ\text{C}$ in dissociation solution (in mM: 90 Na_2SO_4 , 30 K_2SO_4 , 5.8 MgCl_2 , 0.25 CaCl_2 , 10 HEPES, 20 glucose, 0.001% Phenol Red, pH 7.4), and then triturated to obtain a cell suspension (Bourque and Trudeau, 2000), that was subjected to a differential gradient centrifugation to eliminate dead cells and debris. Cells were plated on polyethyleneimine-coated (PEI) coverslips, mounted into an electrophysiology recording chamber and were left to adhere at room temperature for 15 min, then washed under perfusion with physiological saline solution (in mM: 140 NaCl, 5 KCl, 2 MgCl_2 , 2 CaCl_2 , 10 HEPES, 10 glucose, 6 sucrose, pH 7.35 and 305 mOsm) to remove non-attached cells.

Cells were collected individually under RNase-free conditions by using sterile borosilicate patch pipettes. No intracellular pipette solution was used. Each cell was collected by applying light negative pressure to the pipette. The recording chamber was fixed to the stage of an inverted Nikon Eclipse TE-200 microscope. Coverslips were kept under perfusion of physiological saline solution using a gravity flow system (1 ml/min). Once samples were collected, the content of the pipette was transferred immediately into a pre-chilled $200\text{-}\mu\text{l}$ tube containing $6 \mu\text{l}$ of a freshly prepared solution of 20 U of RNaseOUT and 8.3 mM of DTT (Invitrogen) and then frozen immediately until use. Frozen samples were thawed on ice and subjected to the RT reaction as described for total RNA, but using 1.25 μM RH, 100 units M-MLV RT and 20 additional units of RNaseOUT. A first round of PCR was done as mentioned above, but using half of the RT reaction and 27 cycles. A second round of PCR was done using 10% of the first PCR reaction and 28 cycles.

Primers

All primers were designed according to the NCBI GenBank sequence database using Primer3 (http://frodo.wi.mit.edu/cgi-bin/primer3/primer3_www.cgi) as well as Vector NTI software, and synthesized by AlphaDNA (Montreal, QC, Canada). They were tested using the appropriate positive and negative controls. For β -actin, the forward and reverse primers were 5'-ctctttccagccttctctt-3' and 5'-agtaatctcctctgcatcctg-3', respectively (product size 175 pb). For TH, the primers were 5'-GTTCTCAACCT-GCTTCTCTCT-3' and 5'-GGTAGCAATTTCTCTTTGTGT-3'; TH-nested, 5'-GTACAAAACCTCCTCACTGTCTC-3' and 5'-CTTGATTGGAAGGCAATCTCTG-3' (product size 375 pb). For VGLUT2, the primers were 5'-GGGGAAGAGGGGATAAAGAA-3' and 5'-TGGCTTTCTCCTTGATACTTTG-3'; VGLUT2-nested 5'-atctacagggctgctgagaagaa-3' and 5'-gatagtgctgtgtgacatgt-3' (product size 230 pb). Nested primers were the same as the ones used in the RT-mPCR experiments.

Double immunolabeling for electron microscopy

Fifteen day-old pups were deeply anesthetized with sodium pentobarbital (80 mg/kg, i.p.) and fixed by intra-cardiac perfusion of a solution of 3% acrolein in 0.1 M phosphate buffer (PB, pH 7.4),

followed by 4% PFA in the same buffer. The brain was removed, post-fixed by immersion in the PFA solution at 4 °C for 2 h, and washed in PBS. Fifty micrometer-thick transverse sections across the nAcb were cut in PBS with a vibratome, immersed in 0.1% sodium borohydride in PBS for 30 min at room temperature, and washed in this buffer before further processing. After preincubation for 1 h at room temperature in a blocking solution containing 5% normal goat serum and 0.5% gelatin in PBS, sections were incubated for 48 h at room temperature with both mouse monoclonal anti-TH (Sigma) (1:500) and rabbit polyclonal anti-VGLUT2 antiserum (Synaptic Systems, Goettingen, Germany) (1:500) (Anlauf and Derouiche, 2005) antibodies in blocking solution. The monoclonal anti-TH antibody recognizes an epitope present in the N-terminal region of both rodent and human TH (Haycock, 1993), while the polyclonal anti-VGLUT2 antibody was raised against a C-terminal segment of mammalian VGLUT2 (Fujiyama et al., 2001). The VGLUT2 and TH antibodies were then sequentially labeled in this order with the immunogold and the immunoperoxidase technique, respectively. Sections were rinsed in PBS, incubated overnight at room temperature in goat anti-rabbit IgGs conjugated to 1 nm colloidal gold particles (AuroProbe One, Amersham, Oakville, ON, Canada), diluted 1:50 in blocking solution, and the size of immunogold particles was increased by silver enhancement for 15 min with IntenSE kit (Amersham). Sections were then rinsed in PBS, incubated for 1.5 h at room temperature with biotinylated goat anti-mouse IgGs (Jackson) diluted 1:1000 in blocking solution, rinsed in PBS, incubated for 1 h in a 1:1000 solution of streptavidin–HRP (Jackson), washed in PBS and then in 0.05 M Tris–saline buffer (TBS; pH 7.4), incubated for 2–5 min in TBS containing 0.05% DAB and hydrogen peroxide (0.02%), and washed again in TBS to stop the reaction.

Further processing for electron microscopy was as previously described in detail (Riad et al., 2000). In brief, sections were osmicated, dehydrated and flat-embedded in resin between a glass slide and a plastic coverslip (Rinzl, Thomas Scientific, Swedesboro, NJ, USA). After 48 h of polymerization at 60 °C, the coverslips were removed, and the region of interest (nAcb), identified by light microscopy, was excised from the slides and glued at the tip of resin blocks. Ultrathin sections were then cut with an ultramicrotome (Reichert Ultracut S, Leica Canada, St-Laurent, QC, Canada), collected on bare square-meshed copper grids, stained with lead citrate and examined with an electron microscope (Philips CM100, Philips Electronics, St-Laurent, QC, Canada). Immunocytochemical controls included processing as above but without either one or both primary antibodies. Only the expected single labeling was observed when omitting one or the other primary antibody, and no labeling whatsoever in the absence of both of them.

The electron microscopic analysis focused on the core of the nAcb, at transverse levels that correspond to between A 10.8 and 11.28 mm in the stereotaxic atlas of Paxinos and Watson (2005). Material from seven normal and seven 6-OHDA-lesioned rats, aged 15 days, was examined. In both normal and 6-OHDA-lesioned rats, a minimum of 50 electron micrographs per rat were obtained from a narrow area of thin sections less than 10 μm away from the tissue-resin border at working magnifications ranging from 3000–15,000×. The film negatives were scanned (Epson Perfection 3200), converted into a positive picture, adjusted for brightness and contrast with Photoshop (Adobe), and printed at a final magnifications ranging from 7500–37,500×.

Most immunolabeled profiles could then be positively identified as axon varicosities, i.e. axon dilations (>0.25 μm in transverse diameter) containing aggregated small vesicles and often one or more mitochondria, and displaying or not a synaptic membrane specialization (junctional complex). Smaller immunolabeled profiles were assumed to represent intervaricose segments of unmyelinated axons. Only profiles decorated with three or more immunogold particles were considered as immunogold-labeled.

The immunoperoxidase labeling was readily identified as a more or less dense precipitate, often outlining the small vesicles or mitochondria and the membrane of varicosities. In 30 micrographs per rat, printed at a uniform magnification of 30,000× and showing the best morphological preservation, all singly or dually immunolabeled profiles of axon varicosities were counted and categorized as immunopositive for TH alone, for VGLUT2 alone or for both TH and VGLUT2 (TH/VGLUT2). As an equivalent ultrathin section surface ($\pm 1665 \mu\text{m}^2$) was being examined in every rat, the total number of varicosities in the different categories could be merely divided by the number of rats ($n=7$) for the comparison between normal and 6-OHDA-lesioned rats.

Statistical analyses

All data were expressed as group mean \pm S.E.M. Statistical analyses were performed with SigmaStat (Systat Software, Chicago, IL, USA) or GraphPad Prism 4 (La Jolla, CA, USA). *t*-Tests, analyses of variance (one-way ANOVA) and Tukey post hoc tests were used to determine statistical significance. *P* values below 0.05 were considered statistically significant.

RESULTS

Expression of VGLUT2 mRNA in pre- and postnatal ventral mesencephalon

Double *in situ* hybridization against TH and the three VGLUT subtypes was performed in order to detect VGLUT1–3 mRNAs in developing DA neurons *in vivo*. The selectivity of the [³⁵S]VGLUT mRNA probes was validated by evaluating their distribution in autoradiographs from the brain of normal 15 day-old rats. In keeping with previous observations (Boulland et al., 2004; Fremeau et al., 2002; Gras et al., 2002; Herzog et al., 2004b), VGLUT1 mRNA was abundant in the pyramidal cell layer of hippocampus and in cerebral cortex; VGLUT2 mRNA in the red nucleus and the medial geniculate nucleus, and VGLUT3 mRNA in the dorsal and median raphe nuclei (Supplementary online material) (Herzog et al., 2004a). No signal was observed with sense probes (data not shown).

Inspection of these autoradiographs did not show abundant VGLUT2 labeling in the ventral mesencephalon, including the VTA and SN, which could be due to a low sensitivity of detection of our *in situ* hybridization technique, but could also reflect a truly low level of VGLUT2 mRNA at that age (Boulland et al., 2004). However, this did not exclude co-expression by a sub-population of these neurons, or the repression of a broader co-expression at earlier stages of development.

The expression of each VGLUT subtype was therefore examined from E14 to E21 as well as in neonatal rats, using double *in situ* hybridization with Dig-TH and [³⁵S]VGLUT probes. No labeling for VGLUT1 and VGLUT3 mRNA was detected in the mesencephalic region of embryonic or neonatal rats (data not shown). In contrast, at E14–E15 and E16, strong labeling for VGLUT2 mRNA was observed in the region displaying TH mRNA labeling (Fig. 1A, A1), i.e. in the ventral and paramedial zone of the mesencephalon where developing DA neurons are found (Smits et al., 2006). At later embryonic ages (E18–21), TH mRNA labeling remained abundant, but the overlap with VGLUT2 labeling was lost, suggesting a lowering of VGLUT2 expression in dopaminergic

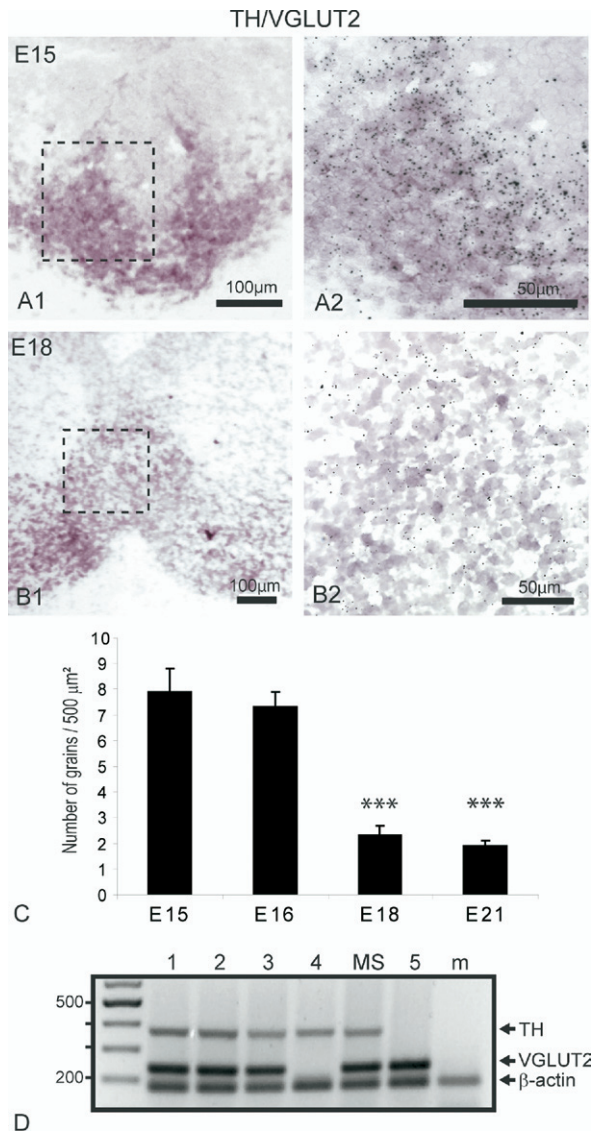


Fig. 1. Selectivity and evaluation of co-expression of TH and VGLUT2 mRNA in prenatal ventral mesencephalon. (A–B1) Double *in situ* hybridization with DIG-labeled probes to detect TH mRNA (purple) and radiolabeled probes to detect VGLUT2 mRNA (silver grains). (A–A1) TH and VGLUT2 mRNAs in the ventral mesencephalon of an E15 rat. Note the strong overlap in regional co-localization of both mRNAs. (B–B1) At E18, there is little overlap in the regional distribution of the two mRNAs. A1 and B1 are enlargements of the areas outlined in dashed line in A and B. (C) Density of VGLUT2 mRNA labeling (number of silver grains per 500 μm² of section) in TH-Dig positive areas of mesencephalic sections from embryos at different ages. Both E18 and E21 values are significantly lower than E15 and E16 values (means ± S.E.M. from three embryos at E15 and E18 and 5 embryos at E16 and E21). *** $P < 0.001$ by ANOVA and Tukey post hoc test. (D) Presence of VGLUT2 mRNA in freshly dissociated mesencephalic DA neurons (cells 1–3) identified by the presence of TH mRNA. Cell 4 only expresses TH mRNA, while cell 5 only expresses VGLUT2. MS, mesencephalon plus striatum used as positive control; m, muscle, used as negative control. For interpretation of the references to color in this figure legend, the reader is referred to the Web version of this article.

gic nuclei (Fig. 1B, B1). Quantification of the VGLUT2 mRNA labeling in TH-Dig-positive regions of embryonic ventral mesencephalon showed averages of 7.9 ± 0.9 and 7.3 ± 0.6

silver grains per 500 μm² of section at E15 ($N=3$) and E16 ($N=5$), respectively, and significant decreases to 2.3 ± 0.4 and 1.9 ± 0.2 per 500 μm² at E18 ($N=3$) and E21 ($N=5$), respectively ($P < 0.001$ by one-way ANOVA and Tukey's multiple comparison post hoc test) (Fig. 1C). To confirm the presence of VGLUT2 mRNA in embryonic DA neurons, single-cell RT-PCR was used in individual E15 DA neurons. After acute dissociation of the ventral mesencephalon from E15 embryos, 54 cells were collected. Of these 54 cells, 13 were found to contain VGLUT2 mRNA and four to contain TH mRNA. Out of these four DA neurons, three were found to contain VGLUT2 mRNA (Fig. 1D), thus confirming the apparent frequent expression of this transcript in embryonic DA neurons.

In postnatal rats, numerous neurons dually-labeled for TH and VGLUT2 mRNAs were visible in the rostral linear raphe (RLi) nucleus (Fig. 2A, B), while only small numbers were observed in the VTA and SNc (Fig. 2C, D). The percentage of DA (TH mRNA) neurons co-expressing VGLUT2 mRNA in the VTA and SN of normal neonatal rats is given in Table 1. In P5, P10 and P15 pups ($N=4$ for each age), we counted a total of 5382 neurons containing TH mRNA in the SN, and 4656 in the VTA. Out of these, only a small subset showed dual labeling (33 in the SN, and 120 in the VTA). There was no statistically significant change in the percentage of dually labeled neurons in the VTA or the SN between these ages (Table 1). At each age, the per-

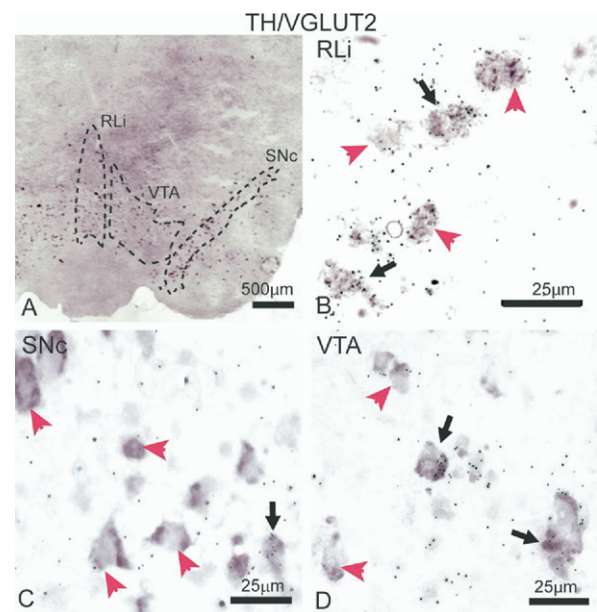


Fig. 2. Co-expression of TH and VGLUT2 mRNA in RLi, VTA or SNc neurons of 15 day-old normal rats. Double *in situ* hybridization with DIG-labeled and radiolabeled probes as in Fig. 1 (TH mRNA in purple, and silver grains for VGLUT2 mRNA). (A, B) Co-expression of VGLUT2 and TH mRNA is observed in a subset of DA neurons (black arrows) in the RLi. Many other neurons displayed only TH mRNA (red arrows). (C, D) A few neurons in the SNc (C) and VTA (D) of normal rats display both mRNAs (black arrows). Red arrows designate neurons containing TH mRNA only. Outlines of VTA, SNc and RLi drawn from Paxinos and Watson (2005). For interpretation of the references to color in this figure legend, the reader is referred to the Web version of this article.

Table 1. Number and proportion of VTA and SN neurons co-expressing TH and VGLUT2 mRNA in postnatal control rats

Control rats	TH+ cells per section	TH+/VGLUT2+ cells per section	TH+/VGLUT2 percent
P5 (N=4)			
VTA	121±14	4.1±1.2	3.4±0.8%
SN	131±10	0.9±0.2	0.7±0.1%
P10 (N=4)			
VTA	158±18	3.8±1	2.4±0.4%
SN	167±19	1.3±0.6	0.8±0.3%
P15 (N=4)			
VTA	102±7	1.8±0.3	1.8±0.3%
SN	152±12	0.7±0.4	0.4±0.2%

Means±S.E.M. for the number of neurons counted per section in four rats at each age (three or four sections per rat). On the right, the number of dually labeled neurons (TH+/VGLUT2+) is expressed as a percentage of all neurons containing TH mRNA (TH+).

centage of co-expression was significantly higher in the VTA (parabrachial and paranigral subdivisions) than the SN ($2.6\pm 0.5\%$ versus $0.6\pm 0.1\%$ in average; $P<0.001$, *t*-test). The highest ratio was observed in the RLi ($24.1\pm 6.4\%$; $N=3$), in which DA neurons are less numerous and dispersed along the midline (Fig. 2A, B). Some neurons expressing VGLUT2 only were also seen in the VTA, suggesting the presence of primarily glutamatergic neurons in this mesencephalic region (e.g. Fig. 4A).

Co-expression of VGLUT2 by DA neurons after neonatal 6-OHDA lesion

The neonatal administration of 6-OHDA allowed us to evaluate the effects of an early injury on the transmitter phenotype of surviving DA neurons. As expected from earlier studies (Fernandes Xavier et al., 1994), 11 days after 6-OHDA (P15), TH immunoreactivity was almost abolished in the dorsal striatum of 6-OHDA rats, but residual labeling persisted in the ventral striatum, and notably in the nAcb (Fig. 3A, B). The consequences of the 6-OHDA lesion on VGLUT2 expression were first investigated by measuring TH, VGLUT2 and β -actin mRNAs in tissue blocks of the VTA and SN of normal, sham and 6-OHDA-lesioned 15 day-old rats ($N=3$), using semi-quantitative RT-PCR. As shown in Fig. 3C and D, TH mRNA was markedly decreased after 6-OHDA compared with normal or sham controls (optical density 0.41 ± 0.04 vs. 1.1 ± 0.04 and 0.87 ± 0.16 for normal and sham respectively; one-way ANOVA, $F(2,8)=12.1$, $P<0.05$). In contrast, there were no significant differences in VGLUT2 mRNA levels between either group (Fig. 3C, D; OD 0.94 ± 0.03 for 6-OHDA rats vs. 0.88 ± 0.03 and 0.82 ± 0.1 for normal and sham rats, respectively; one-way ANOVA, $F(2,8)=0.9$, $P>0.05$).

In view of the major decrease in the number of DA neurons, the lack of a parallel decrease in VGLUT2 mRNA was compatible with either one of two possibilities. The proportion of surviving DA neurons expressing VGLUT2 could be increased following the 6-OHDA lesion, thus compensating for the decrease in DA neuron number, or else, most of the VGLUT2 mRNA that was measured originated from non-DA neurons that were not affected by the lesion.

To distinguish between these possibilities, the number and proportion of DA neurons that expressed VGLUT2 mRNA were determined by double *in situ* hybridization in sham-operated compared with 6-OHDA-lesioned rats. As shown in Table 2, 11 days after the lesion, there was a modest but nonsignificant increase in the number and proportion of dually labeled neurons in the VTA of sham-operated ($N=4$) compared with control rats ($N=4$) (56 TH+/VGLUT2+ over 1124 TH+, i.e. $7.1\pm 1.5\%$ versus 19 TH+/VGLUT2+ over 1116 TH+, i.e. $1.8\pm 0.3\%$), and no change in the SN. As also shown in Table 2, the total number of neurons displaying TH mRNA was considerably reduced in the VTA of the lesioned rats ($N=4$), while such neurons had almost totally disappeared from the SN. Yet, the number of VTA neurons co-expressing TH and VGLUT2 mRNA after 6-OHDA (142 TH+/VGLUT2+ over 530 TH+ neurons) was higher than in control and sham-operated animals (Fig. 4), whereas none were observed in the SN. As the number of

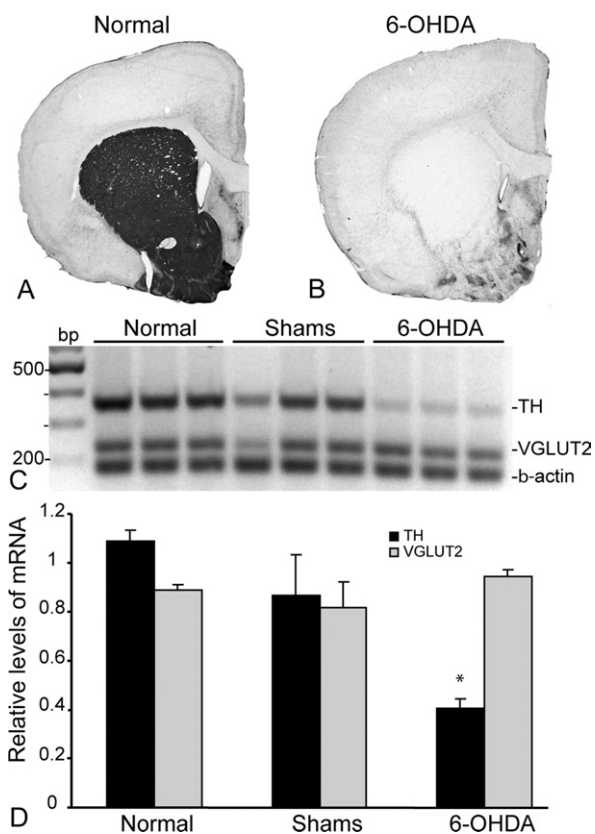


Fig. 3. Effect of the neonatal 6-OHDA lesion on TH and VGLUT2 mRNA levels in the ventral mesencephalon of 15 day-old rats. (A, B) TH immunoreactivity in the P15 rat striatum after i.c.v. injection of aCSF (sham) (A) or 6-OHDA (B). Note that the 6-OHDA lesion induced an almost complete loss of TH levels, confirming the success of the lesion. (C) Expression profile of relative TH, VGLUT2 and β -actin mRNA levels in the mesencephalon of P15 rats. Measurements were made by multiplex semi-quantitative RT-PCR from control, sham-operated and 6-OHDA-lesioned rats (three animals per condition). (D) Histogram representing the relative levels of TH and VGLUT2 mRNA measured from control, sham or lesioned tissue. The data represents the average±S.E.M. from three rats per condition. Values were normalized to the signal obtained for β -actin mRNA levels. * $P<0.05$ when compared with control or sham groups by ANOVA and Tukey post hoc test.

Table 2. Number and proportion of VTA and SN neurons co-expressing TH and VGLUT2 mRNA in sham and 6-OHDA lesioned rats

P15, rats	TH+ cells per section	TH+/VGLUT2+ cells per section	Percent
Shams (N=4)			
VTA	98±7	6.9±2.7	7.1±1.5%
SN	126±13	0.9±0.4	0.7±0.3%
6-OHDA (N=4)			
VTA	39±5	10.3±1	26.3±2.5%***
SN	4.6±2.6	0	0

Data from P15 rats subjected to vehicle (sham) or 6-OHDA injection at P4. As in Table 1, means±S.E.M. for the number of neurons counted per section in four rats of each group. The proportion of dually labeled neurons (TH+/VGLUT2+ over all TH+) is significantly greater in 6-OHDA-lesioned than sham rats.

*** $P<0.001$ by ANOVA and Tukey test post hoc.

VTA DA neurons was markedly reduced by the lesion, this resulted in a highly significant increase in the proportion of dually labeled VTA neurons (26.3±2.5%; Table 2). An ANOVA confirmed the statistical significance of this difference ($P<0.001$ for 6-OHDA versus each other group), in the absence of a significant difference between the sham and control rats.

TH and VGLUT2 containing axon terminals in the nAcb of normal and 6-OHDA-lesioned 15 day-old rats

In every specimen from both normal and 6-OHDA-treated rats examined by electron microscopy after dual immunolabeling for TH and VGLUT2, axon terminals (varicosities) labeled for TH only (DAB), VGLUT2 only (gold particles) and both TH and VGLUT2 could be observed (Fig. 5). A quantification of these results revealed a considerable reduction (38%) in the number of TH positive singly-labeled varicosities after the 6-OHDA lesion compared with normal (Table 3). An apparent reduction in the number of singly labeled, VGLUT2 positive terminals was also measured, but did not reach statistical significance because of the considerable variability between rats. Surprisingly, there was no significant decrease in the number of dually labeled terminals estimated as a proportion of the total number of TH positive terminals after 6-OHDA (Table 3). To the contrary, 37% of residual TH positive terminals in the nAcb of 6-OHDA-lesioned rats were dually labeled, a value which was significantly higher than the 28% measured in normal rats ($P<0.05$). Interestingly, even in single thin sections, the dually labeled terminals frequently showed a synaptic membrane specialization (junctional complex), either asymmetrical or symmetrical (Fig. 5C and 5F). However, a larger sample will be required to determine the relationship between synaptic specializations and transmitter status.

DISCUSSION

While confirming that, in normal rats, a subset of VTA DA neurons expresses VGLUT2 mRNA, this study suggests that this dual transmitter phenotype is more broadly expressed during early than late embryonic development,

and reveals that it may be activated in VTA DA neurons surviving a neonatal 6-OHDA lesion. It also provides the first demonstration of the presence of VGLUT2 protein in TH-immunopositive axon varicosities of the nAcb, reinforcing the possibility of a dual release of glutamate and DA by these nerve terminals *in vivo*.

VGLUT2 expression in mesencephalic DA neurons *in vivo*

The initial goal of the present study was to characterize the glutamatergic phenotype of mesencephalic DA neurons, and to determine whether, as in culture (Dal Bo et al., 2004), these neurons co-express VGLUTs *in vivo*. In agreement with two recent reports (Kawano et al., 2006; Yamaguchi et al., 2007), in normal postnatal rat, only VGLUT2 mRNA was detected in a small sub-population of ventral mesencephalic neurons containing TH mRNA. Therefore, like other monoaminergic neuronal populations expressing a glutamatergic phenotype, such as C1 adrenergic neurons expressing VGLUT2 (Stornetta et al., 2002) and raphe serotonin neurons expressing VGLUT3 (Gras et al., 2002), mesencephalic DA neurons co-express only one VGLUT subtype. Albeit low, the proportion of DA neurons co-expressing VGLUT2 in normal postnatal rat was significantly higher in the VTA than in the SNc. This was in keeping with the recent observations of Kawano et al. (2006) in adult animals, and further highlights phenotypic differences between DA neurons in these two nuclei, as already shown for the levels of expression of TH, DA transporter and calbindin (Rogers, 1992; Blanchard et al., 1994; Korotkova et al., 2004, 2005). The small subset of DA neurons expressing VGLUT2 mRNA in normal postnatal rat contrasted with the high proportion of isolated DA neurons in culture known to release glutamate synaptically (~60%) (Sulzer et al., 1998) or to express VGLUT2 protein (~80%) (Dal Bo et al., 2004), suggesting that VGLUT2 expression might be enhanced in isolated DA neurons *in vitro*.

In vivo, VGLUT2 expression may be abundant and widespread during development but repressed in mature

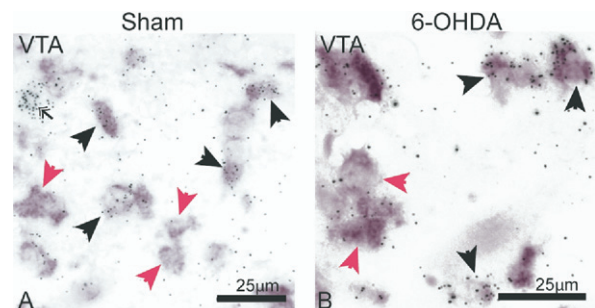


Fig. 4. Co-expression of TH and VGLUT2 mRNA in VTA neurons of 15 day-old sham control (A) or 6-OHDA-lesioned (B) rats. (A, B) Compared with normal (Fig. 2D) and sham control (A), a greater number of VTA neurons co-expressed TH and VGLUT2 mRNA (black arrows) in 6-OHDA-lesioned rats (B). Red arrows designate neurons containing TH mRNA only, and double arrows neurons with VGLUT2 mRNA only. For interpretation of the references to color in this figure legend, the reader is referred to the Web version of this article.

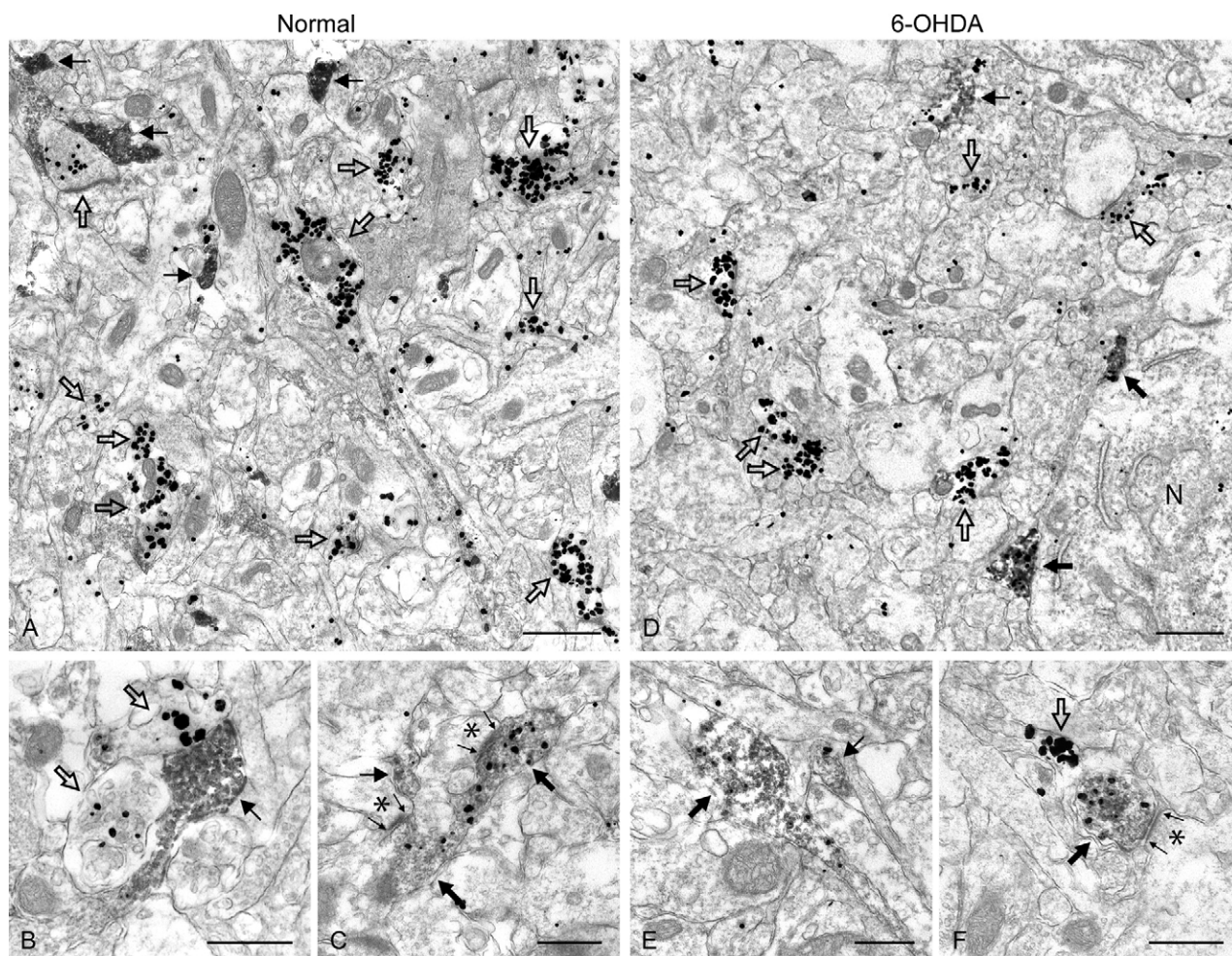


Fig. 5. Electron microscopic visualization of singly (TH or VGLUT2) and doubly (TH/VGLUT2) immunopositive axon terminals (varicosities) in the nAcb of normal (A–C) or 6-OHDA-lesioned (D–F) 15-day old rats. TH and VGLUT2 were respectively labeled with the immunoperoxidase (fine DAB precipitate) and the immunogold technique (dense, silver-intensified, gold particles). At the relatively low magnification of A and D, varicosities labeled for TH only (thin black arrows), VGLUT2 only (empty arrows) or TH and VGLUT2 (thick black arrows) may be observed in the same field. In D, note the presence of two doubly labeled varicosities closely apposed to a neuronal cell body (N in cytoplasm). In B, a triad is formed by three juxtaposed axon varicosities, one of which shows TH labeling only (thin black arrow) and the two others VGLUT2 labeling only (empty arrows). In C, the thick black arrows designate two varicosities along the same axon, which display both TH and VGLUT2 labeling. Both of these varicosities make an asymmetrical synaptic contact (between small arrows) with a dendritic spine (asterisks). In E, a doubly labeled varicosity (thick black arrow) is seen emerging from its parent unmyelinated axon. To its right, a small profile (presumably axonal) is labeled for TH only (thin black arrow). In F, underneath a small profile singly labeled for VGLUT2, a larger, doubly labeled axon varicosity (thick black arrow) forms a symmetrical synaptic contact (between small arrows) with a dendritic spine (asterisk). Scale bars=1 μm (A, D); 0.5 μm (B, C, E, F).

DA neurons. Indeed, at 14–16 embryonic days, VGLUT2 mRNA was strongly and broadly co-expressed with TH mRNA in the region of ventral mesencephalon where DA neurons first develop (Kalsbeek et al., 1988), and no longer detectable at later embryonic stages (E18 and E21). Single-cell RT PCR confirmed the frequent co-expression of VGLUT2 in E15 DA neurons. In rat ventral midbrain at E18, DA neurons are found in the same relative location that they will occupy in the adult brain, and their projections begin to reach the ventro-lateral part of the neostriatum (Specht et al., 1981; Voorn et al., 1988) in which neurogenesis begins (Bayer, 1984). Future work will be needed to verify that the rapid change in regional overlap of TH and VGLUT2 expression in embryonic ventral midbrain does represent a reduced number of DA neurons expressing

VGLUT2 mRNA, and to determine the specific role of this dual phenotype during the growth of these neurons. Rapid declines in VGLUT2 expression have been described previously in postnatal rat brain (Boulland et al., 2004) (see also Danik et al., 2005). They are likely to reflect the repression of a glutamatergic phenotype transiently expressed during critical periods of development.

VGLUT2 expression in DA neurons surviving a neonatal 6-OHDA lesion

Neonatal i.c.v. administration of 6-OHDA is a well-established model to study adaptive and plastic properties of central DA neurons *in vivo* (Fernandes Xavier et al., 1994; Joyce et al., 1996; Penit-Soria et al., 1997; Neal-Beliveau

Table 3. Number of TH, VGLUT2, and TH/VGLUT2 immunopositive axon terminals in the nAcb of 15 day-old normal versus 6-OHDA-lesioned rats

P15 rats	TH+ terminals	VGLUT2+ terminals	TH+/VGLUT2+ terminals	Percent
Normal (N=7)				
N terminals	1125	892	318	28±2%
Mean±S.E.M.	161±8	127±32	45±6	
6-OHDA (N=7)				
N terminals	696	581	256	37±4%*
Mean±S.E.M.	99±11***	88±16	37±4	

N terminals is the total number of immunopositive axon terminals in each category, counted over an equivalent total surface of 11 655 μm^2 of this section (1665 μm^2 per rat) in each group, as explained in Experimental Procedures. The percentage of all TH-labeled axon terminals dually immunolabeled for VGLUT2 is given on the right.

*** $P < 0.001$ by unpaired Student's *t*-test.

* $P < 0.05$ by unpaired Student's *t*-test.

and Joyce, 1999). This lesion destroys most DA neurons in the SNc and decreases the number of DA neurons in the VTA, but, as previously shown, many DA neurons of this latter region survive. The present study revealed that the percentage of VTA DA neurons expressing VGLUT2 mRNA was markedly increased in 15 day-old 6-OHDA lesioned rats compared with normal or sham controls. This increase in number of VTA DA neurons containing VGLUT2 mRNA was far greater than could be explained by a preferential survival of those VTA neurons normally expressing the dual phenotype. Interestingly, an increase in the number and in the proportion of dually labeled DA neurons was already observed 2 days after the surgery, at P6 (96 VGLUT2+/TH+ over 561 TH+ counted in three animals; 17.1 ± 4.4), indicating an early and rapid activation of VGLUT2 expression in surviving DA neurons (data not shown). These data argue in favor of the hypothesis of an induction or derepression of VGLUT2 expression in many of the surviving DA neurons.

The proportion of VTA DA neurons expressing VGLUT2 appeared to be also slightly increased in sham-injected rats that were pre-treated with desipramine to prevent degeneration of noradrenergic neurons. Although this trend did not reach statistical significance, it may have been due to an elevation of extracellular norepinephrine. Interestingly, in adult rat, chronic desipramine treatment has been shown to increase VGLUT1 mRNA in the cerebral cortex and hippocampus (Moutsimilli et al., 2005; Tordera et al., 2005), and VGLUT2 mRNA in the thalamus (Tordera et al., 2005). Preliminary data suggest that a modest increase of VGLUT2 mRNA in the ventral mesencephalon may indeed result from a single injection of desipramine in normal neonatal rats (data not shown).

On the other hand, there was no detectable increase in VGLUT2 mRNA expression in the SNc DA neurons having survived the 6-OHDA lesion. This perhaps reflected a further difference between VTA and SNc DA neurons, not only in their ability to express VGLUT2 under normal conditions, but also in their potential to up-regulate its co-expression after trauma. Experiments in progress should tell whether VTA DA neurons of adult rats retain the potential to express VGLUT2 after partial 6-OHDA lesion. Interestingly, a number of recent reports have described an enhanced expression of VGLUT2 by mature neurons in

response to various stimuli (Kawasaki et al., 2005, 2006; Hrabovszky et al., 2006; Aymerich et al., 2006). These findings illustrate the remarkable plasticity of the glutamate transmitter phenotype of neurons. The recent demonstration that hippocampal granule cells begin to express glutamic acid decarboxylase and to release GABA in addition to glutamate after a kindling protocol (Gutierrez, 2000; Gutierrez and Heinemann, 2006) or in response to glial cell-derived neurotrophic factor (Gomez-Lira et al., 2005) also favors this view. These latter results have been interpreted as the reactivation of a normally repressed developmental program (Seal and Edwards, 2006), which might also be the case for VGLUT2 expression by neonatally-lesioned DA neurons.

Presence of VGLUT2 protein in DA terminals

Considering that mesencephalic DA neurons of the VTA densely innervate the nAcb (Oades and Halliday, 1987), this small nucleus was the ideal anatomical area to search for a colocalization of TH and VGLUT2 protein in axon terminals. After dual immunolabeling for electron microscopy, 28% of TH positive terminals in the core of nAcb could be distinctly visualized as also containing VGLUT2 protein. Such a proportion of axon terminals containing both TH and VGLUT2 protein was much higher than the observed proportion of DA neurons expressing VGLUT2 mRNA, a discrepancy for which several possible explanations could be advanced, in addition to limitations in sensitivity of the dual *in situ* hybridization technique. VGLUT2 positive DA neurons could have established a higher density of axon terminals at this stage of development than DA neurons which do not express VGLUT2. It is also possible that the half-life of the VGLUT2 protein is relatively long, accounting for its persistence many days after interruption of its synthesis and export to axon terminals.

As expected, the 6-OHDA lesion caused a substantial decrease in the number of TH-immunopositive terminals in the nAcb, as evaluated either by dual immunofluorescence or by double labeling immuno-electron microscopy. In the latter material, the 38% decrease in axon terminals labeled for TH was considerably less than the 60% reduction in number of VTA neurons displaying TH mRNA, perhaps reflecting, at least in part, the survival of DA neurons which

no longer expressed detectable amounts of TH mRNA. Interestingly, this diminished number of TH terminals was not accompanied by a statistically significant reduction in the number of dually TH and VGLUT2 positive axon terminals (decrease of less than 20%). On the contrary, there was a small but significant increase in the percentage of all TH terminals which exhibited the dual phenotype (from 28% to 37%; $P < 0.05$). This finding is in line with the increase in the proportion of VTA DA neurons that co-expressed VGLUT2 mRNA after the lesion. Alternatively, it could indicate that axon terminals arising from DA neurons that also contain VGLUT2 were less sensitive to the 6-OHDA-induced degeneration. Because, in many brain regions, central DA neurons are endowed with non-synaptic as well as synaptic axon varicosities (Hattori et al., 1991; Descarries et al., 1996; Ingham et al., 1998), it will be of interest to explore the possible relationship between the glutamatergic phenotype of TH positive terminals and their synaptic versus non-synaptic differentiation.

CONCLUSION

Although the specific role of glutamate in mesencephalic DA neurons remains undetermined, the early developmental expression of VGLUT2 in these neurons suggests an implication of glutamate release in the establishment or fine-tuning of their projections. Further experiments will be required to test this hypothesis more directly and to investigate which signals activate or derepress VGLUT2 expression in lesioned VTA neurons. It will also be of major interest to determine whether such a phenotypic switch may occur in adult animals, as well as the possible role of the dual DA-glutamate phenotype (and its regulation) within the context of pathological states.

Acknowledgments—This work was funded in part by a grant from NARSAD to L.-E.T. and by CIHR grant MOP-3544 to L.D., and also supported by an infrastructure grant from the FRSQ to the GRSNC (Groupe de Recherche sur le Système Nerveux Central). N. B.-C. was recipient of a studentship from the GRSNC. The plasmids used to prepare VGLUT probes were kindly provided by Dr. S. El Mestikawy. The authors wish to thank François Gilbert, Brigitte Paquet and Geneviève Beaudry for their help with the *in situ* hybridization experiments.

REFERENCES

- Aihara Y, Mashima H, Onda H, Hisano S, Kasuya H, Hori T, Yamada S, Tomura H, Yamada Y, Inoue I, Kojima I, Takeda J (2000) Molecular cloning of a novel brain-type Na(+)-dependent inorganic phosphate cotransporter. *J Neurochem* 74:2622–2625.
- Anlauf E, Derouiche A (2005) Astrocytic exocytosis vesicles and glutamate: a high-resolution immunofluorescence study. *Glia* 49:96–106.
- Aymerich MS, Barroso-Chinea P, Perez-Manso M, Munoz-Patino AM, Moreno-Igoa M, Gonzalez-Hernandez T, Lanciego JL (2006) Consequences of unilateral nigrostriatal denervation on the thalamostriatal pathway in rats. *Eur J Neurosci* 23:2099–2108.
- Bayer SA (1984) Neurogenesis in the rat striatum. *Int J Dev Neurosci* 2:163–175.
- Beaudry G, Langlois MC, Weppe I, Rouillard C, Lévesque D (2000) Contrasting patterns and cellular specificity of transcriptional regulation of the nuclear receptor nerve growth factor-inducible B by haloperidol and clozapine in the rat forebrain. *J Neurochem* 75:1694–1702.
- Bellocchio EE, Hu H, Pohorille A, Chan J, Pickel VM, Edwards RH (1998) The localization of the brain-specific inorganic phosphate transporter suggests a specific presynaptic role in glutamatergic transmission. *J Neurosci* 18:8648–8659.
- Blanchard V, Raisman-Vozari R, Vyas A, Michel PP, Javoy-Agid F, Uhl G, Agid Y (1994) Differential expression of tyrosine hydroxylase and membrane dopamine transporter genes in subpopulations of dopaminergic neurons of the rat mesencephalon. *Brain Res Mol Brain Res* 22:29–38.
- Borodinsky LN, Root CM, Cronin JA, Sann SB, Gu X, Spitzer NC (2004) Activity-dependent homeostatic specification of transmitter expression in embryonic neurons. *Nature* 429:523–530.
- Borodinsky LN, Spitzer NC (2007) Activity-dependent neurotransmitter-receptor matching at the neuromuscular junction. *Proc Natl Acad Sci U S A* 104:335–340.
- Boulland JL, Qureshi T, Seal RP, Rafiki A, Gundersen V, Bergersen LH, Fremeau RT Jr, Edwards RH, Storm-Mathisen J, Chaudhry FA (2004) Expression of the vesicular glutamate transporters during development indicates the widespread corelease of multiple neurotransmitters. *J Comp Neurol* 480:264–280.
- Bourque M-J, Trudeau L-E (2000) GDNF enhances the synaptic efficacy of dopaminergic neurons in culture. *Eur J Neurosci* 12:3172–3180.
- Chuhma N, Zhang H, Masson J, Zhuang X, Sulzer D, Hen R, Rayport S (2004) Dopamine neurons mediate a fast excitatory signal via their glutamatergic synapses. *J Neurosci* 24:972–981.
- Cossette M, Parent A, Lévesque D (2004) Tyrosine hydroxylase-positive neurons intrinsic to the human striatum express the transcription factor Nurr1. *Eur J Neurosci* 20:2089–2095.
- Dal Bo G, St-Gelais F, Danik M, Williams S, Cotton M, Trudeau L-E (2004) Dopamine neurons in culture express VGLUT2 explaining their capacity to release glutamate at synapses in addition to dopamine. *J Neurochem* 88:1398–1405.
- Danik M, Cassoly E, Manseau F, Sotty F, Mougnot D, Williams S (2005) Frequent coexpression of the vesicular glutamate transporter 1 and 2 genes, as well as coexpression with genes for choline acetyltransferase or glutamic acid decarboxylase in neurons of rat brain. *J Neurosci Res* 81:506–521.
- Descarries L, Watkins KC, Garcia S, Bosler O, Doucet G (1996) Dual character, asynaptic and synaptic, of the dopamine innervation in adult rat neostriatum: a quantitative autoradiographic and immunocytochemical analysis. *J Comp Neurol* 375:167–186.
- Fernandes Xavier FG, Doucet G, Geffard M, Descarries L (1994) Dopamine neoinnervation in the substantia nigra and hyperinnervation in the interpeduncular nucleus of adult rat following neonatal cerebroventricular administration of 6-hydroxydopamine. *Neuroscience* 59:77–87.
- Fremeau RT Jr, Burman J, Qureshi T, Tran CH, Proctor J, Johnson J, Zhang H, Sulzer D, Copenhagen DR, Storm-Mathisen J, Reimer RJ, Chaudhry FA, Edwards RH (2002) The identification of vesicular glutamate transporter 3 suggests novel modes of signaling by glutamate. *Proc Natl Acad Sci U S A* 99:14488–14493.
- Fremeau RT Jr, Troyer MD, Pahner I, Nygaard GO, Tran CH, Reimer RJ, Bellocchio EE, Fortin D, Storm-Mathisen J, Edwards RH (2001) The expression of vesicular glutamate transporters defines two classes of excitatory synapse. *Neuron* 31:247–260.
- Fujiyama F, Furuta T, Kaneko T (2001) Immunocytochemical localization of candidates for vesicular glutamate transporters in the rat cerebral cortex. *J Comp Neurol* 435:379–387.
- Furshpan EJ, MacLeish PR, O'Lague PH, Potter DD (1976) Chemical transmission between rat sympathetic neurons and cardiac myocytes developing in microcultures: evidence for cholinergic, adrenergic, and dual-function neurons. *Proc Natl Acad Sci U S A* 73:4225–4229.
- Gillespie DC, Kim G, Kandler K (2005) Inhibitory synapses in the developing auditory system are glutamatergic. *Nat Neurosci* 8:332–338.

- Gomez-Lira G, Lamas M, Romo-Parra H, Gutierrez R (2005) Programmed and induced phenotype of the hippocampal granule cells. *J Neurosci* 25:6939–6946.
- Gras C, Herzog E, Belenchi GC, Bernard V, Ravassard P, Pohl M, Gasnier B, Giros B, El Mestikawy S (2002) A third vesicular glutamate transporter expressed by cholinergic and serotonergic neurons. *J Neurosci* 22:5442–5451.
- Gratto KA, Verge VM (2003) Neurotrophin-3 down-regulates trkA mRNA, NGF high-affinity binding sites, and associated phenotype in adult DRG neurons. *Eur J Neurosci* 18:1535–1548.
- Gutierrez R (2000) Seizures induce simultaneous GABAergic and glutamatergic transmission in the dentate gyrus-CA3 system. *J Neurophysiol* 84:3088–3090.
- Gutierrez R, Heinemann U (2006) Co-existence of GABA and Glu in the hippocampal granule cells: implications for epilepsy. *Curr Top Med Chem* 6:975–978.
- Hattori T, Takada M, Morizumi T, Van der Kooy D (1991) Single dopaminergic nigrostriatal neurons form two chemically distinct synaptic types: possible transmitter segregation within neurons. *J Comp Neurol* 309:391–401.
- Haycock JW (1993) Multiple forms of tyrosine hydroxylase in human neuroblastoma cells: quantitation with isoform-specific antibodies. *J Neurochem* 60:493–502.
- Herzog E, Belenchi GC, Gras C, Bernard V, Ravassard P, Bedet C, Gasnier B, Giros B, El Mestikawy S (2001) The existence of a second vesicular glutamate transporter specifies subpopulations of glutamatergic neurons. *J Neurosci* 21:RC181.
- Herzog E, Gilchrist J, Gras C, Muzerelle A, Ravassard P, Giros B, Gaspar P, El Mestikawy S (2004a) Localization of VGLUT3, the vesicular glutamate transporter type 3, in the rat brain. *Neuroscience* 123:983–1002.
- Herzog E, Landry M, Buhler E, Bouali-Benazzouz R, Legay C, Henderson CE, Nagy F, Dreyfus P, Giros B, El Mestikawy S (2004b) Expression of vesicular glutamate transporters, VGLUT1 and VGLUT2, in cholinergic spinal motoneurons. *Eur J Neurosci* 20:1752–1760.
- Hisano S, Hoshi K, Ikeda Y, Maruyama D, Kanemoto M, Ichijo H, Kojima I, Takeda J, Nogami H (2000) Regional expression of a gene encoding a neuron-specific Na(+)-dependent inorganic phosphate cotransporter (DNPI) in the rat forebrain. *Brain Res Mol Brain Res* 83:34–43.
- Hrabovszky E, Kalló I, Turi GF, May K, Wittmann G, Fekete C, Liposits Z (2006) Expression of vesicular glutamate transporter-2 in gonadotrope and thyrotrope cells of the rat pituitary. Regulation by estrogen and thyroid hormone status. *Endocrinology* 147:3818–3825.
- Ingham CA, Hood SH, Taggart P, Arbuthnott GW (1998) Plasticity of synapses in the rat neostriatum after unilateral lesion of the nigrostriatal dopaminergic pathway. *J Neurosci* 18:4732–4743.
- Jackson D, Bruno JP, Stachowiak MK, Zigmond MJ (1988) Inhibition of striatal acetylcholine release by serotonin and dopamine after the intracerebral administration of 6-hydroxydopamine to neonatal rats. *Brain Res* 457:267–273.
- Joyce JN, Frohna PA, Neal-Beliveau BS (1996) Functional and molecular differentiation of the dopamine system induced by neonatal denervation. *Neurosci Biobehav Rev* 20:453–486.
- Joyce MP, Rayport S (2000) Mesoaccumbens dopamine neuron synapses reconstructed in vitro are glutamatergic. *Neuroscience* 99:445–456.
- Kalsbeek A, Voorn P, Buijs RM, Pool CW, Uylings HB (1988) Development of the dopaminergic innervation in the prefrontal cortex of the rat. *J Comp Neurol* 269:58–72.
- Kawano M, Kawasaki A, Sakata-Haga H, Fukui Y, Kawano H, Nogami H, Hisano S (2006) Particular subpopulations of midbrain and hypothalamic dopamine neurons express vesicular glutamate transporter 2 in the rat brain. *J Comp Neurol* 498:581–592.
- Kawasaki A, Hoshi K, Kawano M, Nogami H, Yoshikawa H, Hisano S (2005) Up-regulation of VGLUT2 expression in hypothalamic-neurohypophysial neurons of the rat following osmotic challenge. *Eur J Neurosci* 22:672–680.
- Kawasaki A, Shutoh F, Nogami H, Hisano S (2006) VGLUT2 expression is up-regulated in neurohypophysial vasopressin neurons of the rat after osmotic stimulation. *Neurosci Res* 56:124–127.
- Korotkova TM, Ponomarenko AA, Brown RE, Haas HL (2004) Functional diversity of ventral midbrain dopamine and GABAergic neurons. *Mol Neurobiol* 29:243–259.
- Korotkova TM, Ponomarenko AA, Haas HL, Sergeeva OA (2005) Differential expression of the homeobox gene Pitx3 in midbrain dopaminergic neurons. *Eur J Neurosci* 22:1287–1293.
- Lavin A, Nogueira L, Lapish CC, Wightman RM, Phillips PE, Seamans JK (2005) Mesocortical dopamine neurons operate in distinct temporal domains using multimodal signaling. *J Neurosci* 25:5013–5023.
- Moutsimilli L, Farley S, Dumas S, El Mestikawy S, Giros B, Tzavara ET (2005) Selective cortical VGLUT1 increase as a marker for antidepressant activity. *Neuropharmacology* 49:890–900.
- Neal-Beliveau BS, Joyce JN (1999) Timing: A critical determinant of the functional consequences of neonatal 6-OHDA lesions. *Neurotoxicol Teratol* 21:129–140.
- Ni B, Wu X, Yan GM, Wang J, Paul SM (1995) Regional expression and cellular localization of the Na(+)-dependent inorganic phosphate cotransporter of rat brain. *J Neurosci* 15:5789–5799.
- Oades RD, Halliday GM (1987) Ventral tegmental (A10) system: neurobiology. 1. Anatomy and connectivity. *Brain Res* 434:117–165.
- Paxinos G, Watson C (2005) The rat brain in stereotaxic coordinates. San Diego: Academic Press.
- Penit-Soria J, Durand C, Hervé D, Besson MJ (1997) Morphological and biochemical adaptations to unilateral dopamine denervation of the neostriatum in newborn rats. *Neuroscience* 77:753–766.
- Puma C, Danik M, Quirion R, Ramon F, Williams S (2001) The chemokine interleukin-8 acutely reduces Ca(2+) currents in identified cholinergic septal neurons expressing CXCR1 and CXCR2 receptor mRNAs. *J Neurochem* 78:960–971.
- Riad M, Garcia S, Watkins KC, Jodoin N, Doucet E, Langlois X, El Mestikawy S, Hamon M, Descarries L (2000) Somatodendritic localization of 5-HT1A and preterminal axonal localization of 5-HT1B serotonin receptors in adult rat brain. *J Comp Neurol* 417:181–194.
- Rogers JH (1992) Immunohistochemical markers in rat brain: colocalization of calretinin and calbindin-D28k with tyrosine hydroxylase. *Brain Res* 587:203–210.
- Seal RP, Edwards RH (2006) Functional implications of neurotransmitter co-release: glutamate and GABA share the load. *Curr Opin Pharmacol* 6:114–119.
- Smits SM, Burbach JP, Smidt MP (2006) Developmental origin and fate of meso-diencephalic dopamine neurons. *Prog Neurobiol* 78:1–16.
- Specht LA, Pickel VM, Joh TH, Reis DJ (1981) Fine structure of the nigrostriatal anlage in fetal rat brain by immunocytochemical localization of tyrosine hydroxylase. *Brain Res* 218:49–65.
- Stachowiak MK, Bruno JP, Snyder AM, Stricker EM, Zigmond MJ (1984) Apparent sprouting of striatal serotonergic terminals after dopamine-depleting brain lesions in neonatal rats. *Brain Res* 291:164–167.
- St-Hilaire M, Landry E, Lévesque D, Rouillard C (2005) Denervation and repeated L-DOPA induce complex regulatory changes in neurochemical phenotypes of striatal neurons: implication of a dopamine D1-dependent mechanism. *Neurobiol Dis* 20:450–460.
- Stornetta RL, Sevigny CP, Guyenet PG (2002) Vesicular glutamate transporter DNPI/VGLUT2 mRNA is present in C1 and several other groups of brainstem catecholaminergic neurons. *J Comp Neurol* 444:191–206.
- Sulzer D, Joyce MP, Lin L, Geldwert D, Haber SN, Hattori T, Rayport S (1998) Dopamine neurons make glutamatergic synapses in vitro. *J Neurosci* 18:4588–4602.

- Tordera RM, Pei Q, Sharp T (2005) Evidence for increased expression of the vesicular glutamate transporter, VGLUT1, by a course of antidepressant treatment. *J Neurochem* 94:875–883.
- Trevino M, Gutierrez R (2005) The GABAergic projection of the dentate gyrus to hippocampal area CA3 of the rat: pre- and postsynaptic actions after seizures. *J Physiol* 567:939–949.
- Varoqui H, Schafer MK, Zhu H, Weihe E, Erickson JD (2002) Identification of the differentiation-associated Na⁺/PI transporter as a novel vesicular glutamate transporter expressed in a distinct set of glutamatergic synapses. *J Neurosci* 22:142–155.
- Voorn P, Kalsbeek A, Jorritsma-Byham B, Groenewegen HJ (1988) The pre- and postnatal development of the dopaminergic cell groups in the ventral mesencephalon and the dopaminergic innervation of the striatum of the rat. *Neuroscience* 25:857–887.
- Yamaguchi T, Sheen W, Morales M (2007) Glutamatergic neurons are present in the rat ventral tegmental area. *Eur J Neurosci* 25:106–118.
- Yang B, Slonimsky JD, Birren SJ (2002) A rapid switch in sympathetic neurotransmitter release properties mediated by the p75 receptor. *Nat Neurosci* 5:539–545.

APPENDIX

Supplementary data associated with this article can be found, in the online version, at doi: [10.1016/j.neuroscience.2008.07.032](https://doi.org/10.1016/j.neuroscience.2008.07.032).

(Accepted 15 July 2008)
(Available online 25 July 2008)